micromachines

MDPI

Article

Microfluidics Integration on GaAs acoustic biosensors with a Leakage-Free PDMS and High Pressure based on Bonding Technology

Saber Hammami [1,*], Aleksandre Oseev [1], Sylwester Bargiel [1], Rabah Zeggari [2], Céline Elie-Caille [1], and Thérèse Leblois [1,*]

1 FEMTO-ST Institute, CNRS UMR-6174, Université de Bourgogne Franche-Comté, 25030 Besançon, France
2 FEMTO Engineering, 15B Avenue des Montboucons, 25030 Besançon, France
* Correspondence: saber.hammami@femto-st.fr, therese.leblois@femto-st.fr

Abstract: Microfluidics integration of acoustic biosensors is an actively developing field. Despite significant progress in "passive" microfluidic technology, integration with microacoustic devices is still in research state. The major challenge remains the bonding of polymers with monocrystalline piezoelectrics to seal the microfluidic biosensors. In this contribution we specifically address the challenge of microfluidics integration with gallium arsenide (GaAs) acoustic biosensors. We have developed a robust plasma-assisted bonding technology allowing strong connection between PDMS microfluidic chip and GaAs/SiO_2 at low temperature (70°C) and low applied pressure. Mechanical and fluidic performances of fabricated device were studied. The bonding surfaces were characterized by water contact angle measurement, ATR-FTIR, AFM and SEM analysis. The bonding strength was characterized using a tensile machine and pressure/leakage tests. The study showed that the sealed chips were able to achieve a limit- of bonding strength of 2.06 MPa. The adhesion of PDMS to GaAs was significantly improved by use of SiO_2 intermediate layer, permitting the bonded chip to withstand at least 8 bar of burst pressure. The developed bonding approach can be a valuable solution for microfluidics integration of several types of MEMS devices.

Keywords: microsystems; microfluidics; acoustic biosensor; bonding technology; PDMS-SiO_2/GaAs bonding; Leakage test

Citation: Lastname, F.; Lastname, F.; Lastname, F. Title. *Micromachines* **2022**, *13*, x. https://doi.org/10.3390/xxxxx

Academic Editor: Firstname Lastname

Received: date
Accepted: date
Published: date

1. Introduction

Microfluidics field has emerged as a solution for precise control and manipulation of fluids at a microliter scales [1–3]. On-chip microfluidics integration is one of the most promising development vectors in particular in the field of biosensors [4,5]. Microfluidics integrated lab-on-a-chip solutions have been widely used in many applications, such as clinical diagnostics on human physiological fluids, cell biology [6], detection of tumor cells, biochemical detections, electrophoresis, biochemistry, PCR [7], DNA analysis, single-cell trapping, droplets microfluidics [8], biosensors and more [9]. Recently introduced microfluidic biosensors have the advantages of portability, high precision, easy application, and high-throughput parallel processing [10]. Ma et al. [11] showed that microfluidic channel could lower down the detection limit of endotoxin with the confined space and enhance Van der Waals force. Zhang et al. [12] used microfluidic channel with biosensor for detection of Salmonella using Fe-nanocluster amplification and smart phone imaging.

Micromachining processes open up the possibility to combine micro-sensors and microfluidics onto a single chip. Various sensing technologies have been integrated in microfluidic systems (e.g. optical, conductive, acoustic, radio frequency and other) making possible to assess physical properties of bio-analytes on a chip level. Ability to complete

an assessment directly on a chip is a distinguishing feature of lab-on-a-chip solutions comparing to widely spread bio-analytical tools such as surface plasmon resonance (SPR).

The integration of biosensors with microfluidics circuits is in the core of the development of integrated bio-analytical chips. Among all existing approaches, acoustic biosensors become an important tool to study molecular interactions at the surface. The acoustic biosensors have been widely studied in the detection of gases and liquids [13,14]. There are different types of acoustic biosensor approaches that were developed during the last decades. Bulk acoustic wave devices (BAWs) became one of the most successful approaches in the field.

There are several materials that can be used in the fabrication of acoustic wave sensors. GaAs has been shown to be very well suited for biosensing application [15–17]. GaAs is a microtechnical material that combines piezoelectric properties and the possibilities for devices integration and miniaturization. GaAs can be batch micromachined using Inductive Coupled Plasma Reactive Ion Etching as well as using low-cost wet chemical etching [18,19] . Beside its beneficial microfabrication facilities, GaAs surface can be chemically functionalized with alkanethiols [20] silanes and phosphonates [21] . The microfluidics integration of GaAs BAWs has a potential to introduce a novel sensing platform.

Microfluidics solutions on the other hand are used to be built based on materials such as silicon, glass, PMMA. These materials are commonly used to manufacture fluidic channels, taking advantage of their good mechanical properties and easiness of surface modification to immobilize affinity tags for binding of target molecules on surfaces. Based on PDMS elastomers became attractive alternative materials for microfluidics due to low cost and their remarkable physical and chemical properties, such as wide temperature range, low stiffness, chemical inertness, biocompatibility, rapid prototyping, optical transparency, non-reactivity, high gas permeability. These features make PDMS a potential material for various applications such as pattern transfer, as well as for fabrication of the complex microfluidics systems [22,23] . In addition, its low bonding temperature (lower than 100°C) makes it an excellent material for bonding elastomer substrates since many elastomer substrates cannot withstand a high bonding temperature.

Reproducible bonding/sealing remains one of the highest challenges for reliable applications of microfluidic systems in biosensors. The popular bonding methods such as anodic bonding for Si/Glass microfluidic devices, thermo-compression bonding or chemical assisted bonding [24–26] encounter various difficulties when applied for piezoelectric substrates. On the other hand, polymers provide the alternative solutions for microfluidics packaging. Recently, several new strategies were introduced to improve microfluidics packaging for the integrated sensor solutions. According to the literature, Kersy et al. used the adhesion promotor GE SS4120, while it does not improve adhesion of PDMS to Teflon [27]. It deceases the adhesion strength between PDMS-PDMS. However, this method improves adhesion of PDMS to silicon, glass and aluminum, only allows the formation of a strong bond between the substrate and an un-structured layer of PDMS. Carlos Luis et al. [28] have proposed the use of narrow electrode connectors for minimizing the solution leakage in the PDMS-Au interface. Yong et al. [29] have used thermo-compression and laser bonding to fabricate multi-layer glass microfluidic chips. Application of sticky elastomer was introduced for epidermal electronics [30–32] . Heterogeneous crosslinking of PDMS was applied to enhance adhesion of PDMS to several substrates as seen in Jeong et al. [33] . Plasma-assisted bonding was used by Xi et al. [34] for improve the bonding between PDMS-coated glass cover plate and silicon substrate.

In the current contribution, we develop the solution for microfluidics integration of GaAs biosensors. In particular, we study PDMS-GaAs system where the challenge raises due to GaAs being inert to plasma bonding. To address the challenge, some authors have attempted to increase the adhesion between the PDMS and the substrate by using a gold layer. However, this method is not suitable to seal patterned PDMS with micromachined GaAs. Others have proposed 3-aminopropyl)trimethoxysilane (APTES) and achieved a bonding strength of 406 kPa for PMMA/PDMS bonding [35,36]. A thermal bonding

method is used to bond four-layer microfluidic chip [37]. In the other approach, PDMS is mixed with a small amount of polyethylenimine solution to prepare a sticky thin layer, which works like a sticky tape to adhere on glass, PMMA, and metal by contact press [38]. Lastly, Anil et al, [39] have developed microfluidics-integrated microscale that comprise an isoporous nanostructured membrane. The GaAs on Ge/Si substrate was first flipped with the GaAs nanopyramids side bonded to a Polydimethylsiloxane (PDMS) substrate, whereas a transparent flexible polymer film was weakly bonded by Van der Waals force [40,41]. The SiO_2 layer was used to increase PMMA bonding capability to PDMS in fabricating gas micro valves. Ahmad et al, have showed strong and irreversible bond of PDMS on PMMA when it is covered with SiO_2 nano particles [42].

In this study, we developed the approach for irreversible and leakage-free plasma assisted bonding to integrate PDMS microfluidic channel with GaAs substrate. For this purpose, we combine thin-film SiO_2 intermediate layer on GaAs substrate with plasma O_2 treatment and low-temperature annealing. In brief, this bonding technology is obtained in four main steps: 1) SiO_2 deposition, 2) plasma O_2 treatment, 3) chip alignment and bonding, and 4) annealing at low temperature 70°C. This method is appealing for its compatibility to traditional replication method using PDMS and the surface structures can be retained. The characterization of PDMS and GaAs/SiO_2 surfaces before bonding was verified by contact angle, Attenuated Total Reflectance-Fourier Transformed Infrared Spectroscopy (ATR-FTIR), AFM and the SEM analysis. Bonded chips were characterized using a tensile machine strength bonding equipment on PDMS and a leakage bench test.

2. Materials and Methods

2.1 Materials

Polydimethylsiloxane (PDMS, Sylgard 184) was obtained from Dow Corning Toray Corp. SU-8 3025 photoresist was purchased from MicroChem (Newton, MA, USA). Undoped, 3-inch in diameter and 625 ±25 μm thick double-side polished GaAs (100) ± 0.5◦ wafers (AXT, Inc., Fremont, CA, USA) were used to fabricate the biointerface chips. Acetone (ACP Chemicals, Saint-Léonard, QC, Canada) were used to clean substrates. Red color dye was purchased from Shanghai Macklin Biochemical Co., Ltd. (Shanghai, China). Syringe pump LSP02-1B (Longer Pump, China) was applied to generate constant flow rate in microfuidic chip. Diamond saw dicing was used to cut PDMS for placing microfuidic chip. SEM microscope (Thermofisher APREO S Low-vacuum SEM and 30 mm^2 SDD EDX) was used to observe in detail the microfuidic channel. AFM scans of different dimensions were recorded in order to have a representative sampling of the surface roughness of GaAs/SiO_2. The AFM cantilever had a nominal resonance frequency of 330 kHz, a force constant of 42 N/m, a length of 125 μm, and a mean width of 30 μm.

2.2 Methods and equipment

The fabrication process of the PDMS microfluidic channel is schematically illustrated in figure 1. SU-8 mold of 70μm in thickness was fabricated with SU-8 3050 onto a 1mm-thick silicon wafer using standard photolithography processes including spin coating, pre-baking, exposure, post-baking and development. The SU-8 mold was then used to replicate PDMS microfluidic channel. PDMS with thickness of 3 mm was prepared by pouring the mixture of low-modulus PDMS (component ratio A:B = 1:10, Sylgard 184, Dow Corning).

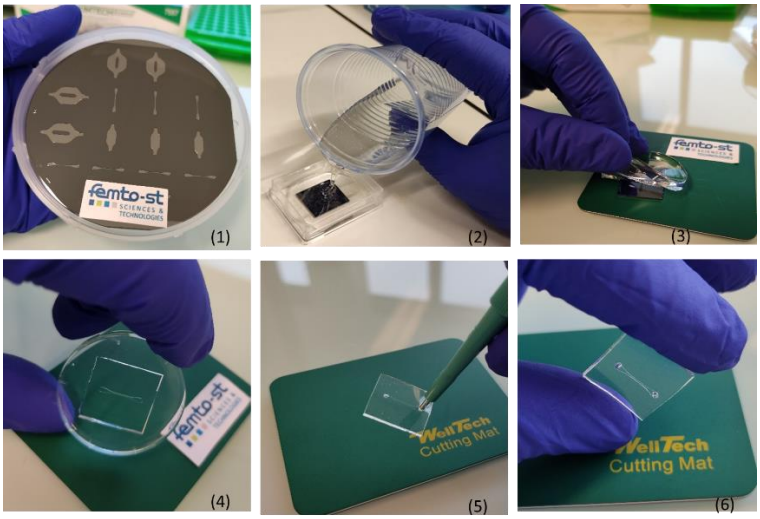

Figure 1. Fabrication process of the PDMS microfluidic channel by replica moulding: (1) fabrication of SU8 master mold using photolithography; (2) Pouring of the mixture of PDMS prepolymer and curing agent into the master mould and allowing it to solidify; (3), (4) Peeling of the solidified PDMS from the master mould and cutting; (5) Punching the inlet and outlet holes; (6) Microfluidic channel.

Air bubbles that appeared during the mixing were removed using a vacuum desicator, followed by baking at 80 °C for 2 h, followed by pouring onto the SU-8 mold to have a sticky layer of about 300 μm. Finally, the prepared PDMS structures were peeled off from the mold and small inlet and outlet holes were punched. Images of the SU-8 mold and the fabricated PDMS microfluidic channel are shown in figure 1. The resulting channels have a hight of 60 μm and a width of 300 μm. The GaAS surface was covered with the SiO_2 layer by RF reactive magnetron sputtering MP450S machine (Plassys, France). Plasma activation process was performed in 15mTorr, parameters like power 150 W, oxygen flow 80 sccm.

Figure 2 presents an experimental setup to measure flow rate and pressure in the microfluidic channel. Once the devices were fabricated and assembled, we connected 25 mL syringes to Tygon (Sigma-Aldrich) tubing to control the volume of air pumped in and out the control channels. A syringe pump is mounted to accurately displace the syringe plunger. Additionally, we connected the inlet of the microfluidic device with Tygon tubing to a supplementary syringe pump to control the flow rate of our medium and cell sample. In our experiments, the syringe volume varies from 0 mL to 25 mL.

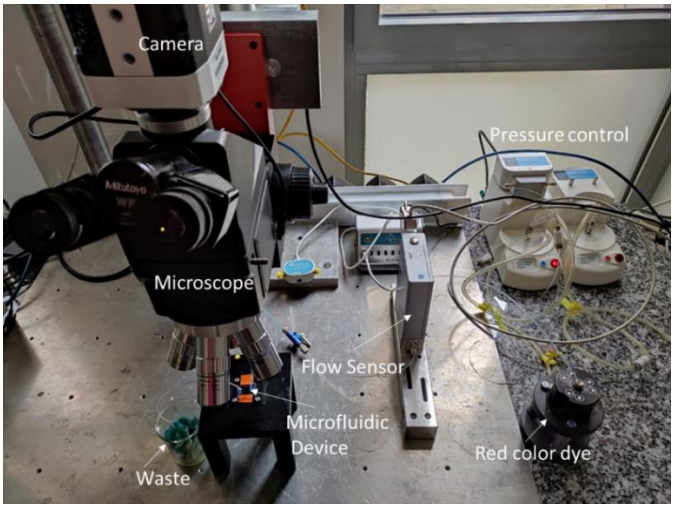

Figure 2. Experimental setup to control flow rate and pressure in the microfluidic channel.

Hence, the pressure difference varies from 0 to 8 bar. With the syringe pumps, the single-layer valves in this device can be accurately controlled without using more complicated electropneumatic systems. An LG16 (Sensirion) microfuidic control system was used to deliver fluid to the channel of the test device and to monitor the applied pressure. Images of the microfluidic channel were obtained with optical microscope (Mitutoyo FS70, Mitutoyo Corp., Kawasaki, Japan) and a camera (IDS μEye, IDS Imaging Development Systems, Obersulm, Germany) with a spatial resolution of 5.5 μm/pixel. During our experiments, a flow sensor connected to a PC is placed for continuous recording of the flow rate and pressure flow in the microfluidic channel.

3. Results

3.1. SEM Characterization

The test PDMS microfluidic structure about 3mm in thickness was cut along the channel length by a sharp blade. Resulted PDMS membrane with exposed microchannel (see figure (3A) was coated with Cr thin layer to be analyzed in the SEM microscope. As shown in figure (3B), the shape of a 400μm-wide microchannel pattern casted in PDMS in a single millimeter scale is well preserved.

To show that presented bonding method can preserve the channel profile as pure PDMS does, we bonded a PDMS microfluidic structure to a 650 μm thick, (100) oriented GaAs substrate, previously covered with 100nm SiO_2 layer. Figure (3C) shows the cross-sectional profile of the 80μm-high microchannel after bonding, proving that our way of chip packaging with sandwich structure is safe. The two subtrates (GaAs and PDMS) are covalent bonded after plasma oxygen treatment of SiO_2 intermediate thin layer and thermal annealing.

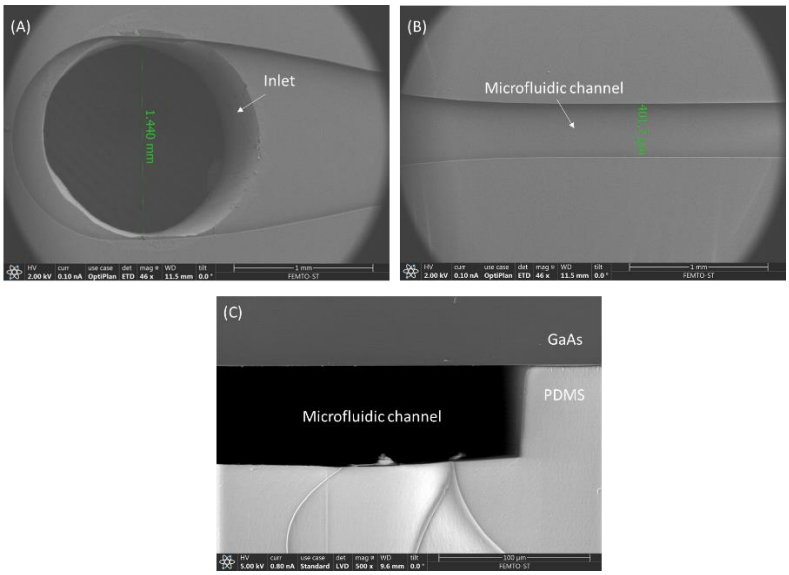

Figure 3. Characterization of microfluidic channels, by SEM: A) General view on PDMS membrane with channel and intlet/outlet holes, (B) microfluidic channel, and (C) cross section of GaAs/SiO_2 bonded to PDMS.

3.2. Activation-Characterization of PDMS and GaAs/SiO_2 surfaces- interfaces

The hydrophobicity of PDMS is associated with the organic methyl groups present in the chemical structure of PDMS. The microchannel was cut out of the mold, following by oxygen plasma treatment to render the PDMS surface hydrophilic. We prepared our bonding technology by a combination of surfaces treatment and annealing (figure 4). Oxygen plasma treatment shows to be the most rapid process to increase of the hydrophilicity of PDMS surface by removing hydrocarbon groups and introducing polar silanol (Si-

OH) groups via oxidation. The activation process duration was 60 seconds. Subsequently, two surfaces were bonded by bringing them into contact under pressure 2N followed by a heat treatment at 70°C for 1 h.

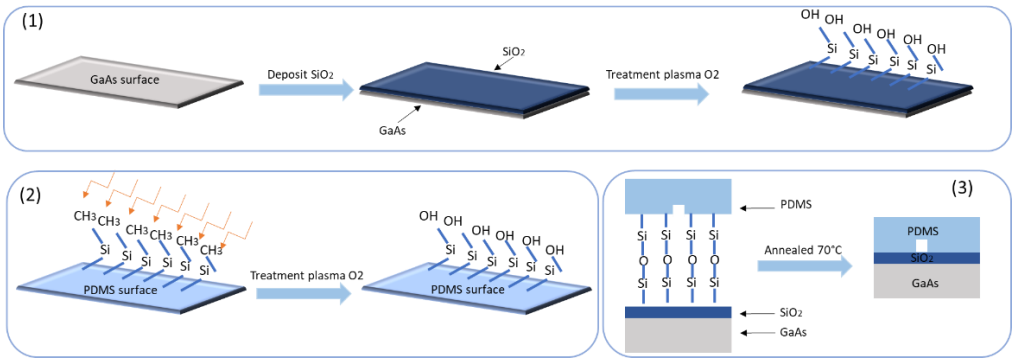

Figure 4. (1) and (2) Schematic presentation of GaAs/SiO_2 and PDMS surfaces modifications by plasma O_2 of, (3) Bonding structure and annealing at 70°C.

To characterize the surfaces modification of PDMS replica and GaAs/SiO_2 substrate after each step of plasma treatment, the contact angles (CA) measurements were performed. Water droplets (5µL) were deposited on the surface of each studied surface. As shown in figure 5, after the surface activation, the contact angle has dropped from 100◦ to 53.8◦ after the oxygen plasma treatment of PDMS, and from 41,3◦ to 11,9° after the oxygen plasma-treated GaAs/SiO_2. The drastic decrease of contact angles indicated that the hydrophobic surface of PDMS became hydrophilic due to the hydroxyl terminals on the plasma-activated PDMS surface. The surface of PDMS after plasma treatment has low surface energy due to the weak intermolecular forces between the methyl groups and the strong (Si–O) and flexible (Si–O–Si) siloxane chain [43].

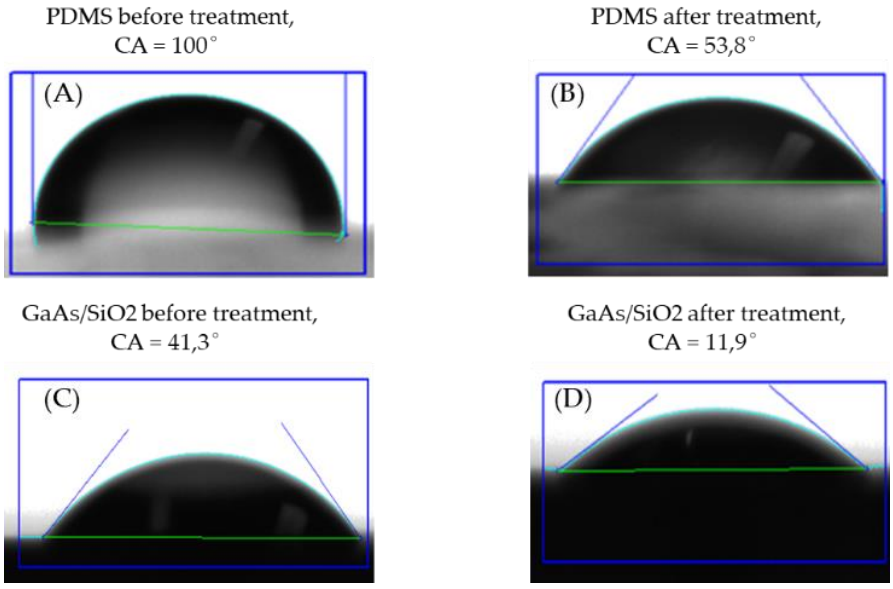

Figure 5. Contact angles for water droplet on the different surfaces, (A) PDMS before treatment, (B) PDMS activated with plasma treatment, (C) GaAs/SiO_2 before plasma O_2 and (D) after plasma O_2 treatment

The surface functional group of GaAs, silicone dioxide and PDMS were analyzed by using ATR-FTIR in the MIR spectral region from 4000 to 500 cm^{-1} (λ=2.5-20µm) in order to

study the effect of oxygen plasma on surface modification. The IR transmittance spectra are presented in figure 6. The peaks between 2,950 cm^{-1} and 2,970 cm^{-1} correspond to the asymmetric Si–OH bonds of PDMS. The peaks at 1,257 cm^{-1} and 1,010 cm^{-1} are attributed to CH_3 asymmetric deformation and Si–O–Si asymmetric deformation of PDMS respectively. A high transmittance on the PDMS substrate in a visible light domain is attained. In comparison, the transmittance of the PDMS substrate is 96%, and that of the GaAs/SiO_2 is 85%, which leads the PDMS transmittance to be 11% better than the GaAs/SiO_2.

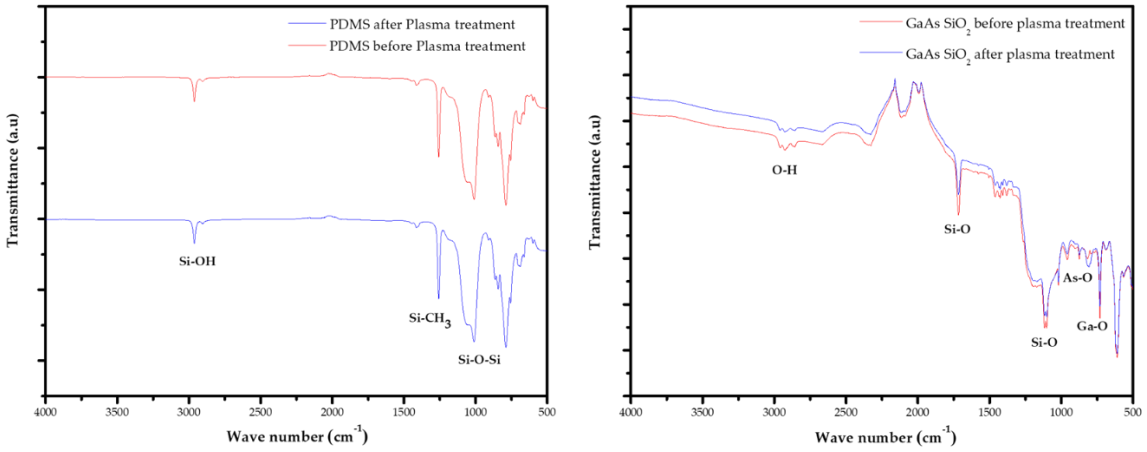

Figure 6. ATR-FTIR spectra recorded from: (a) PDMS polymer before and after plasma treatment, (b) the GaAs/SiO_2 (100) surface before and after plasma treatment.

To ensure the success of surface modification, ATR-FTIR measurement was conducted for six different substrates to verify reproducibility with a maximum error of 5%. Due to the wafer thickness of 650 µm, the GaAs disks support only internal reflections. Especially around 1200 cm^{-1}, silicon oxide possesses a vibrational mode, and thus reduced transparency in the so-called molecular fingerprint region. The presence of peak in 1116 cm^{-1} corresponds to a thin layer of Si-O. Beside the transmittance peak in 1018 cm^{-1} which relates to methyl groups there is trace of chloroform in the silicon dioxide intermediate layer. After the treatment of the oxygen plasma, a large amount of hydroxyl groups are produced in the surfaces of both the silicon dioxide and the PDMS. The later conformal contact of the two surfaces will yield a large amount of Si-O-Si bonds, which will form the strong adhesion between the two surfaces. A reorganization of the short polymeric chains supporting the creation of polar groups can be considered resulting in an increase in temperature. One major advantage of the temperature increase is that the polymerization takes place while preserving the functionality of the monomer. Moreover, the increased cross-linking density in the PDMS directly influences the strength of covalent bonding.

3.2. Optimization of the Bonding microfluidic channel with GaAs substrate.

3.2.1. Test with Plasma O_2 and annealing

The surface of GaAs at different fabrication steps was analyzed with AFM within a scanning area of 3µm* 3µm. The surface morphology of the silicon dioxide was examined using the AFM, in which the grain sizes can be clearly observed and it is noticed that the surface roughness was 0.696 nm. As it can be seen from the AFM images (shown in figure 7(A) and 7(B)), the grain size is in the range of 20 - 58 nm.

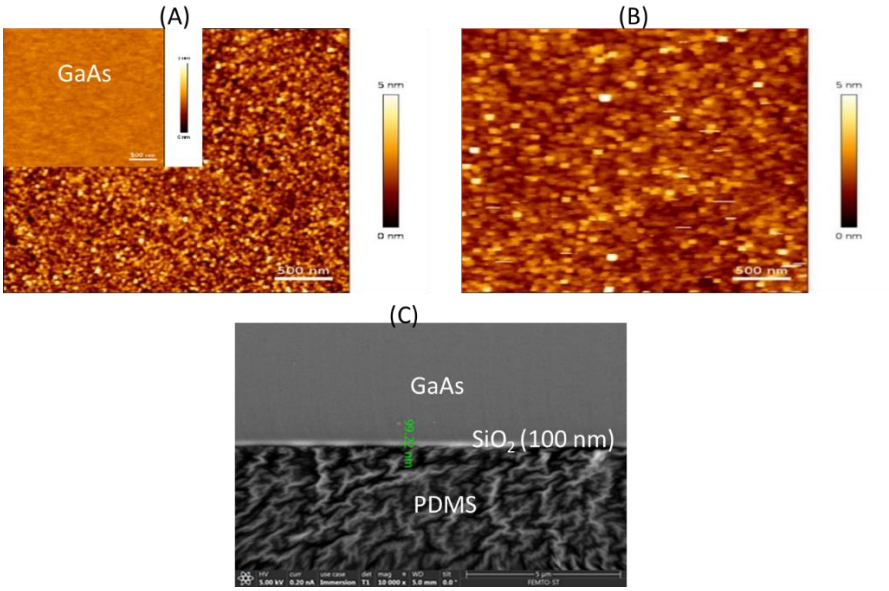

Figure 7. Surface morphology of SiO_2 thin film deposited on GaAs substrates a) before and b) after O_2 plasma treatment (AFM images, 3x3 μm², contact mode, silicon nitride tips (0.32 N/m), 512*512 pixels resolution) c) SEM image of bonding interface (scale 5 μm).

It was found that the average roughness Ra of SiO_2 surface has decreased from 552 pm to 441pm (Table 1) after plasma treatment. It is seen that both the average roughness and root mean square roughness of the PDMS surface are a factor around 465% higher than those of the GaAs/SiO_2.

Table 1. The root mean square Roughness Rq and the average roughness Ra values to various substrates. (PDMS value from literature [44])

Sample	RMS Roughness Rq	Average Roughness Ra
GaAs/SiO_2	709 pm	552 pm
GaAs	114 pm	90 pm
GaAs/SiO_2 after plasma O_2	697 pm	441 pm
PDMS	1441 pm	not reported
PDMS treated by plasma O_2	40031 pm	not reported

Obtained results indicate that smoother surface of GaAs/SiO_2 can be achieved by performing the above-mentioned modification. However, it was shown by Zahid et al. [44] that the plasma O_2 treatment of PDMS leads to a significant increase of its surface roughness, from Rq=1441 pm of freshly PDMS to Rq=40031 pm after plasma treatment. The results further confirmed that the PDMS layer adhered on the silicon dioxide wafer during the cast molding process.

3.2.2 Bonding strength evaluation

The bonding strength was investigated using destructive mechanical tensile test method on square 10x10mm² bonded pair. Beside the GaAs/SiO_2-PDMS bonding configuration, the bonding strength of two other interesting systems, PDMS-Glass and PDMS-$LiNbO_3$ was evaluated. The PDMS, glass and $LiNbO_3$ substrates were cut using diamond saw dicing whereas the GaAs/SiO_2 were cut with a cleavage method. The all substrates were cleaned with acetone and isopropanol to remove dust and organic contaminants. The bonding strenght between the different substrates and PDMS was determined using a mechanical tester for micro-components (Nordson DAGE 4000Plus), equipped with a 250kg cartridge (50kg range used). The specific horizontal setup of the tensile test and the

assembled sample are shown in figure (8A). Two steel sample holders were used to sandwich the bonded sample in between. The upper part of PDMS replica and the backside of all substrates were glued on steel sample holders using a single component instant adhesive Loctite 480 (Henkel Adhesives). The sandwiched sample and its holders were fixed horizontally in the special stud-pull fixture of the tester that eliminates side forces due to gimbal construction. During the tensile test, the motorized stage moved horizontally at a uniform speed of 10 μm/s, while the load force and displacement were recorded simultaneously until failure occurred. Failure mode was determined by optical inspection of fracture surface (interface). The tensile strength of the tested sample was calculated by dividing the measured maximal load force at the bond failure.

All tensil, tests were conducted on the samples that undergone plasma treatment and thermal annealing at 70°C for one hour. The load force curves for all tested configurations are presented in the figure 8(B-left) showing that the bonding strength of GaAs/SiO_2-PDMS is consistently higher when compared to other configurations with $LiNbO_3$ and glass substrates, i.e. 20.34kg, 13.05kg and 7.93kg, respectively. The use of intermediate bonding layer to PDMS substrate increased the bonding strength most significantly: increase of 55% compared with glass substrate and of 156 % compared with $LiNbO_3$. The achieved bonding strength of PDMS and GaAs/SiO_2 to PDMS is ~ 2.06 MPa. For all samples, the strength response exhibits conventional behavior: increase over time until reaching the broken and sharply decreases. The breaking was observed at 12s, 18s and 19s for GaAs/SiO_2, $LiNbO_3$ and glass respectively.

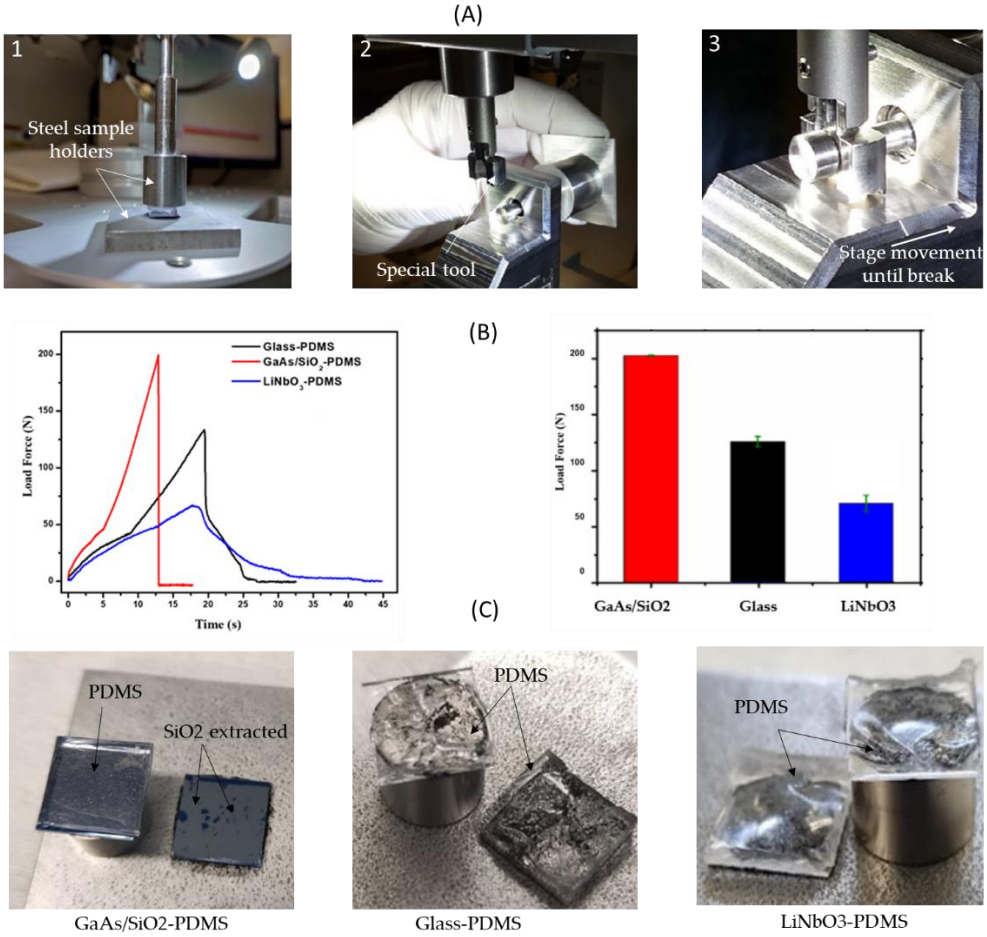

Figure 8. Bonding strength evaluation: (A) Setup of the tensile test: (1) assembly of the bonded sample: the sample is fixed on two steel sample holders, die is places inside the cap rod is screwed into the block and the die is glued between support plate and block, (2) position of the tool behind stud pin (3) the sample mounting for setup of the tensile test. (B-left) Load-time curves obtained for all

substrates bonded to PDMS, (B-right) reproducibility histogram for bonding strength. (C) Photos of broken interface for the PDMS-GaAs/SiO_2, PDMS-Glass and PDMS- $LiNbO_3$.

Figure 8 (B-right), shows the average bonding strength for different samples bonded by the presented process. A good reproducibility for our measurements was observed, with a maximum error of 6% caused by the dispersive imprecision on the dimensions of the bonding area. Figure 8 (C), shows photos of broken structures after the tensile test. In the case of GaAs/SiO_2-PDMS chip, failure was generally observed on the SiO_2-PDMS bonding interface. But in the case of Glass and $LiNbO_3$ samples, failure was observed in the PDMS volume were in good agreement with literature reports [27] [36] [45]. The result can be explained by the higher bonding strength between PDMS-Glass and PDMS-$LiNbO_3$ than the breaking point of cured PDMS materials. In fact, when two amorphous surfaces are brought into contact at elevated temperatures where the molecular chain mobility is high, adhesion occurs at the interface. The chain ends penetrate to the opposite substrate of the interface in the surface layer, leading to high bonding strength. Also, the increase in the surface roughness enhances the adhesion property of substrates, the surface roughness of $LiNbO_3$ was larger than glass no matter what the plasma activation time was according the findings of Xu et al [46]. To go further in our interpretation, we would like to hypothesize the large mismatch in the coefficient of thermal expansion between $LiNbO_3$ and glass (14.4 (x, y-axis)- 7.5 (z-axis) × 10^{-6} K^{-1} for $LiNbO_3$, and 0.56 × 10^{-6} K^{-1} for glass) will produce large thermal stress at the bonding interface may lead to has a significant influence on the value of load force between glass end $LiNbO_3$ [46][47].

Since the SiO_2 layer was also locally detached from the GaAs surface, this failure mode is partially affected by limited adhesion of SiO_2 layer on GaAs that indicates that the bonding strength is higher than the coherence of PDMS material. The high stiffness of GaAs promotes interface failure. Moreover, the high value of the Young's modulus of GaAs (118 GPa) implies that the fracture takes place at the interface.

3.2.3 Leakage tests

In order to validate a leakage-free performance of the bonded GaAs/SiO_2-PDMS chips, the channel inlet/outlet holes were equipped with epoxy-sealed connectors and the leakage test was done under defined flow conditions figure (9A). The flow rate was increased from 10µl/min to 4000µl/min by an increment of 10 µl/min every 30s, looking for the maximum working pressure with no leakage appeared. A red dye solution was used for easier optical microscope inspection of potential leakage at the border of the channel.

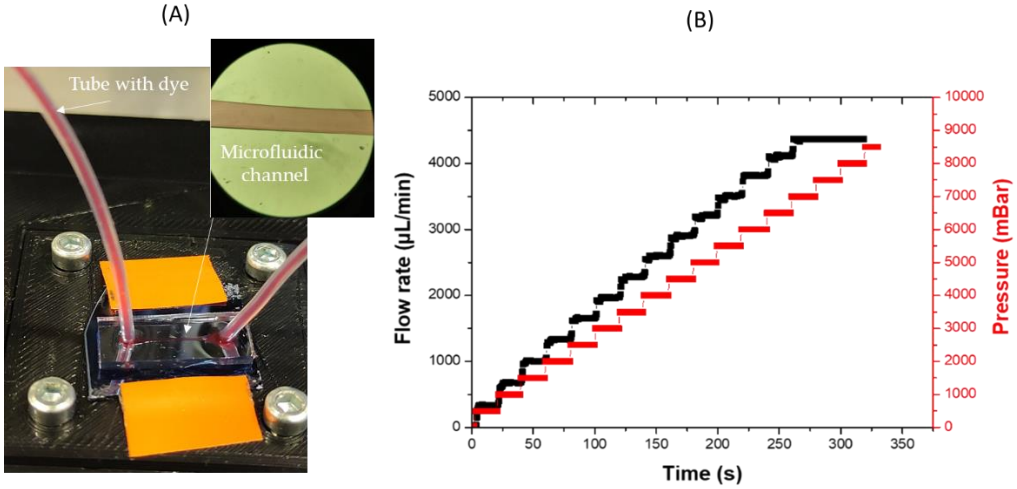

Figure 9. (A) Image of single microfluidic channel (height=60µm, witdh 300µm, length 3cm) infused with a red dye at 3000 µl/min and 5000 mbar pressure, (B) Increase of working pressure and flow rate on the microchannel.

In the leakage test, the design chips based PDMS-SiO_2/GaAs were kept intact (i.e. without dissemination of red dye solution into the bonded interface) until 8 bar of working pressure, maximum available in our experimental setup. It is clearly seen in figure (9A) that the channel is well defined and no leakage is observed at flow rate of 4000µl/min and 8000mbar. The maximum working pressure and the maximum flow rate until the red dye are shown in figure (9B).

4. Discussion

Due to the challenges related to the use of PDMS as the structural material, most studies have focused on finding alternative materials. Although other polymers, such as PS, PMMA, TPE, COP, and photoresists have been used for fabrication of microfluidic devices [45][48-50]. Many different problems releated to the bonding of the microfluidic channel on piezoelectric substrate like GaAs (100) were identified. Bonding processes are required for assembly of microfluidic devices, made of two or more components. This can be achieved by using of double-sided tape, glues, or solvent bonding [51]. The bonding of PDMS on different substrates have been reported in the scientific literature [36], but the solvents used in the bonding process can also strongly influence the growth of cells cultured in the microfluidic devices [52]. Wu et al. used (3-Mercaptopropyl) trimethoxysilane (MPTMS) which was a chemical coupling reagent to modify the surfaces of the noble metals and the PDMS to improve their adhesion [53]. Yong et al. proposed a novel approach to fabricate multi-layer glass microfluidics chips which comprises laser cutting and thermocompression bonding [29]. Among the methods presented above, special treatments processes or the processes of adding additional chemical reagents are required to achieve PDMS adhesion. This work presents an approach to assess how to improve PDMS / GaAs bonding based on the combination of low temperature (<100°C) plasma/thermal treatments and the use of appropriate intermediate bonding layer. We proposed a new solution for bonding of PDMS microfluidic cell on the gallium arsenide substrate, covered with silicon dioxide thin intermediate layer. The aim of the characterization step was to optimize the bonding quality of the multilayer GaAs/SiO_2-PDMS. The study consisted on experimental investigations. We have characterized the bonding interface by various measurement techniques (MEB, AFM, ATR-FTIR, CA).

In order to prove the usefulness of the proposed solution, the elements and the chemical bonds on the PDMS surfaces have been determined by ATR-FTIR analysis. The roughness and topography of various treated and non-treated PDMS and GaAs/SiO_2 surfaces were also analyzed using AFM. The GaAs/SiO_2-PDMS samples fabricated according the proposed method were able to withstand the load force until 20,34 kg without failure, which corresponds to bonding strength of 2,06 MPa which was the highest value we got. This is substantially higher than the bonding strength of other tested microfluidic systems, such as Glass-PDMS or $LiNbO_3$-PDMS. According to the literature it is reasonable to consider the tensile strength of PDMS which is much higher than this bonding breaking point [54]. An analysis system was created to measure the bonding strength of the bonded chips. Zhen et al. showed a bonding strength of over 1.4 MPa for PDMS and PMMA [36]. Yong et al. reported the optimal pressure 0.4 MPa [29]. Kersey et al. employed that the adhesion promoter GE SS4120 can improve the adhesion of PDMS to silicon, glass and aluminum substrates, with bonding strength values 0.841 MPa, 0.847 MPa and 0.488 MPa respectively [27]. From our experiment the bonding strength obtained is higher. In addition, in terms of time consumption, our method was at least times faster than other bonding methods.

In the plasma treatment process, there is only a small amount of hydroxyl groups (the inherent hydroxyl groups) on the surfaces of PDMS and silicon dioxide layer. Xiangdong et al, mentioned that the contact of such two surfaces will produce a small amount of Si-O-Si bonds, which can only form a week adhesion force [55]. Temperature was used to improve the adhesion performance of the bonding technology. Annealing contributes to the stabilization of the bonding layer, improving the cross-linking density in the PDMS

and favorized the orientation molecular chains. For silicon, glass substrates, bonding temperature over 100°C, but for polymer substrates, this would greatly affect the bonding performance. Winnie et al. [56] have used hot embossing technique for bonding PDMS-PMMA substrate at 90°C for 3 hours. A temperature of 605°C was used to bond five-layers of glass microfluidic devices. An additional annealing at 65°C for 1 hours on the PDMS and PS surfaces improved bonding and allowed stabilization of the higher SEF for a longer period of time ((>3 days). In this work, to enhance the bonding, we have combined plasma treatment and annealing. At our experiment after plasma treatment, both parts are aligned and pressed together while completing the curing process at low temperature 70°C for 1 hour. Pre-stress uniformly applied during bonding influences significantly the orientation of the polymer chains. Hammami el al. [57] showed that the combination of temperature and stretch promotes the orientation of molecular chains in the dielectric elastomer. Subsequently the combination of temperature and small deformation promotes bonding of our system. The bonding strength of the adhesive sandwiched between the PDMS and the GaAs/SiO_2 substrates remained the same, even after six months.

The chip holder ensures that leakage only occurs at the bounded interface between the PDMS and GaAs/SiO_2 substrates, i.e., not at the tubing connector. When the leakage was observed, the bonding strength between the PDMS/substrates chip could then be determined. When comparing the strength of our method with GaAs/SiO_2-PDMS and anodic bonding [58] and the rapid Pyrex glass bonding, the strength of our bonding was higher than that of the anodic bonding, are higher than that of the rapid Pyrex bonding. No leak was observed in the tested GaAs/SiO_2-PDMS samples until maximal available working pressure of 8 bar. To our knowledge, it's the highest leakage-free pressure reported in the literature for PDMS-based bonding systems. A comparison between previously reported results of leakage test is shown in Table.2.

Table 2. Maximum pressures obtained from previously reported methods are also shown for comparison.

Sample	PDMS [bar]	Method	Ref
GaAs	≧8	plasma O_2, SiO_2, annealed	This work
Glass	5.1	plasma oxygen ICP	[49]
PDMS	6.7	plasma oxygen RIE	[48]
SU-8	1.5	plasma oxygen, small amount of PEIE and temperature	[38]
Glass/Au	2.38	plasma oxygen and narrow electrode	[28]
TPE	4.7	plasma oxygen and thermal bonding	[59]
PMMA	2.5	plasma oxygen	[44]

Overall, this study presents a method for evaluating whether PDMS can be used as a reliable structural material for microfluidic devices in order to enhance the performance of acousto-fluidics-biosensors based on GaAs. Our contribution is discussed only in terms of basic technological challenge to coupled PDMS with GaAs. Nevertheless, presented results characterizations are likely to contribute to the improvement of the performance of the microfluidics systems combining PDMS and GaAs.

5. Conclusions

We have presented a novel combination between GaAs and PDMS which has would enable the development of an increasingly in-demand array of new applications, including those requiring high flow rates and high pressures. The combination of SiO_2 intermediate layer plasma oxygen and low-temperature annealing and SiO_2 intermediate layer

significantly improves bonding of PDMS to GaAs substrate. In our acoustic biosensor application, one can assume a maximum pressure driving around 8 bar for the fluid. The bonding area of microfluidic devices can withstand a stress about 2.06 MPa. Additionally, this bonding method does not require wet chemical treatment of bonded surfaces which may be prohibited in some application. Bonding features were evaluated using different methods, bonding strength and leakage test. Compared to the previous studies, our bonding method has shown a robust and rapid fabrication technology as well as superior bonding strength and leakage-free pressure. The obtained results can be valuable for research and development of integrated microfluidic devices based on PDMS material in general.

Author Contributions: Conceptualization, S.H, Methodology, S.H, Software: S.H; S.B (for tensil test), Investigation, S.H, Validation, S.H;A.O; Formal analysis, S.H. S.B and C.E-C.; Writing-original draft, S.H.; Writing-review and editing, S.H.,A.O;S.B;R.Z,C.E-C and T.L; Visualisation, S.H.,A.O.;S.B.R.Z;C.E-C and T.L.; Supervision, C.E-C and T.L.; Project administration, T.L; Funding acquisition T.L. All authors have read and agreed to the published version of the manuscript.

Funding: This research was funded by MiMedi (Microtechniques for Innovative Medicines) project funded by BPI France (grant no. DOS0060162/00) and the European Union through the European Regional Development Fund of the Region Bourgogne-Franche-Comte (grant no. FC0013440).

Acknowledgments: The authors would like gratefully thank to Prof. Skandar Basrour from (TEMA Lab-Univ Grenoble Alpes, France) for discussion and Lilia Arapan research engineering (MIMENTO technology centre, Besançon, France) for assistance in clean room. This work was partly supported by the French RENATECH network and its FEMTO-ST technological facilities.

Conflicts of Interest: The authors declare no conflict of interest.

References

1. S, Anderson; B, Hadwen; C, Brown. Thin-film-transistor digital microfluidics for high valuein vitrodiagnostics at the point of need. *lab Chip* **2021**, *21*, 962–975.
2. H, Lu; O, Caen; J, Vrignon; E, Zonta; Z, El Harrak; P, Nizard; J-C, Baret; V, Taly. High throughput single cell counting in droplet-based microfluidics. *Sci Rep*. **2017**, *7*, 1366.
3. P,Neužil; S, Giselbrecht; k, Länge; T-J, Huang; A, Manz. Revisiting lab-on-a-chip technology for drug discovery. *Nat. Rev. Drug Discovery* **2012**, *11*, 620–632.
4. S, Chen; M-H, Shamsi. Biosensors-on-chip: A topical review. *J Micromech Microeng*. **2017**, *27*, 083001.
5. P, Yager; T, Edwards; E, Fu; k, Helton; K, Nelson; M-R, Tam; B-H, Weigl. Microfluidic diagnostic technologies for global public health. *Nature* **2006**, *442*, 412–418.
6. B-G, Abdallah; C, Kupitz. P, Fromme. A, Ros. Crystallization of the large membrane protein complex photosystem i in a microfluidic channel. *ACS Nano* **2013**, *7*, 10534–10543.
7. D, Wu; J, Qin; B, Lin. Electrophoretic separations on microfluidic chips. *J. Chromatogr. A* **2008**, *1184*, 542–559.
8. H, Song; JD, Tice; RF, Ismagilov. A Microfluidic System for Controlling Reaction Networks in Time. *Angew Chemie Int Ed*, **2003**, *42*, 768–772.
9. J, Kim; AS, Campbell; B-E-F, de Ávila; J, Wang. Wearable biosensors for healthcare monitoring. *Nat Biotechnol*. **2019**; *37*, 389–406.
10. K-K, Liu, R-G, Wu; Y-J, Chuang; H-S, Khoo; S-H, Huang; F-G, Tseng. Microfluidic systems for biosensing. *Sensors* **2010** *10*, 6623–6661.
11. W, Ma; L, Liu; Y,Xu; L, Wang. L, Chen; S, Yan; L, Shui; Z, Wangf; S, Li. A highly efficient preconcentration route for rapid and sensitive detection of endotoxin based on an electrochemical biosensor. *Analyst* **2020**, *145*, 4204–4211.
12. H, Zhang; L, Xue; F, Huang; S, Wang; L, Wang; N, Liu; J, Lin. A capillary biosensor for rapid detection of Salmonella using Fe-nanocluster amplification and smart phone imaging. Biosens Bioelectron. **2019**, *127*, 142–149.

13. V, Raimbault; D, Rebiére; C, Dejous; M, Guirardel; J-L, Lachaud. Molecular weight influence study of aqueous poly(ethylene glycol) solutions with a microfluidic Love wave sensor. *Sensors Actuators B. Chem*. **2010**, *144*, 318–322.
14. W, Jakubik; M, Urbańczyk. Hydrogen detection in surface acoustic wave gas sensor based on interaction speed. In Proceedings of the IEEE Sensors, Vienna, Austria, 24-27 Oct. 2004
15. V,Lacour; C, Elie-Caille; T, Leblois; J-J, Dubowski. Regeneration of a thiolated and antibody functionalized GaAs (001) surface using wet chemical processes. *Biointerphases* **2016**, *11*, 019302.
16. J, Chawich; W-M, Hassen; C, Elie-Caille; T, Leblois; J-J, Dubowski. Regenerable ZnO/GaAs bulk acousticwave biosensor for detection of Escherichia coli in "complex" biological medium. *Biosensors* **2021**, *11*, 145.
17. D-T , Marquez; J, Chawich; W-M, Hassen; K, Moumanis; MC, Derosa; J-J Dubowski. Polymer Brush-GaAs Interface and Its Use as an Antibody-Compatible Platform for Biosensing. *ACS Omega* **2021**, *6*, 7286–7295.
18. F, Joint; C, Abadie; P-B, Vigneron; L, Boulley; F, Bayle; N, Isac; A, Cavanna; E, Cambril; E, Herth. GaAs manufacturing processes conditions for micro- and nanoscale devices. *J. Manuf. Process.* **2020**, *60*, 666–672.
19. A, Bienaime; L, Liu; C, Elie-Caille; T, Leblois. Design and microfabrication of a lateral excited gallium arsenide biosensor. *Eur. Phys J. Appl. Physics, EDP Sci.* **2012**, *57*, 21003.
20. O, Voznyy; J-J, Dubowski. Adsorption kinetics of hydrogen sulfide and thiols on GaAs (001) surfaces in a vacuum. *J. Phys. Chem. C*. **2008**, *112*, 3726–3733.
21. H, Sharma; K, Moumanis; J-J, Dubowski. pH-Dependent Photocorrosion of GaAs/AlGaAs Quantum Well Microstructures. *J. Phys. Chem C*. **2016**, *120*, 26129–26137.
22. A-M, Lowe; B-H, Ozer; G-J, Wiepz; P-J, Bertics; N-L, Abbott. Engineering of PDMS surfaces for use in microsystems for capture and isolation of complex and biomedically important proteins: Epidermal growth factor receptor as a model system. *Lab Chip.* **2008**, *8*, 1357–1364.
23. R, Seghir R; S, Arscott. Extended PDMS stiffness range for flexible systems. *Sens Actuators, A*. **2015**, *230*, 33–39.
24. M, Antfolk; C, Antfolk; H, Lilja; T, Laurell; P, Augustsson. A single inlet two-stage acoustophoresis chip enabling tumor cell enrichment from white blood cells. *Lab Chip.* **2015**,*15*, 2102–2109.
25. A, Urbansky; A, Lenshof; J, Dykes; T, Laurell; S, Scheding. Affinity-bead-mediated enrichment of CD8+ lymphocytes from peripheral blood progenitor cell products using acoustophoresis. *Micromachines.* **2016**, *7*, 101.
26. N-C, Nayak; C-Y, Yue; Y-C, Lam; Y-L, Tan. Thermal bonding of PMMA: Effect of polymer molecular weight. Microsyst Technol. **2010**, *16*, 487–491.
27. L, Kersey; V, Ebacher; V, Bazargan; R, Wang; B, Stoeber. The effect of adhesion promoter on the adhesion of PDMS to different substrate materials. *Lab Chip*. **2009**, *9*, 1002–1004.
28. C-L, Gonzalez-Gallardo; A, Díaz Díaz; J-R, Casanova-Moreno. Improving plasma bonding of PDMS to gold-patterned glass for electrochemical microfluidic applications. *Microfluid Nanofluidics.* **2021**, *25*, 20.
29. Y, Han; Z, Jiao; J, Zhao; Z, Chao; Z, You. A simple approach to fabricate multi-layer glass microfluidic chips based on laser processing and thermocompression bonding. *Microfluid Nanofluidics.* **2021**, *25*, 77.
30. K-S, Lee; R-J, Ram. Plastic-PDMS bonding for high pressure hydrolytically stable active microfluidics. *Lab Chip*. **2009**, *9*, 1618–1624.
31. L, Du; M-G, Allen. Silica hermetic packages based on laser patterning and localized fusion bonding. In Proceedings of the IEEE Micro Electro Mechanical Systems, Belfast, UK, 21-25 Jan. 2018.
32. L, Du; M-G, Allen. CMOS Compatible Hermetic Packages Based on Localized Fusion Bonding of Fused Silica. *J Microelectromech Syst.* **2019**, *28*, 656–665.
33. S-H, Jeong; S, Zhang; K, Hjort; J, Hilborn; Z, Wu. PDMS-based elastomer tuned soft, stretchable, and sticky for epidermal electronics. *Adv Mater*. **2016**, *28*, 5830–5836.

34. X, Shu; H, Liu; Y, Zhu; B, Cai; Y, Jin; Y, Wei; F, Zhou; W, Liu; S, Guo. An improved bulk acoustic waves chip based on a PDMS bonding layer for high - efficient particle enrichment. *Microfluid Nanofluidics.* **2018**, *22*, 32.
35. M-E, Vlachopoulou; A, Tserepi; P, Pavli; P, Argitis; M, Sanopoulou; K, Misiakos. A low temperature surface modification assisted method for bonding plastic substrates. *J Micromech Microeng.* **2009**, *19*, 015007.
36. Z, Zhu; P, Chen; K, Liu; C, Escobedo. A Versatile Bonding Method for PDMS and SU-8 and Its Application towards a Multifunctional Microfluidic Device. *Micromachines.* **2016**, *7*, 230.
37. X,Chen; J, Shen; M, Zhou. Rapid fabrication of a four-layer PMMA- based microfluidic chip using CO2 -laser micromachining and thermal bonding. *J Micromech Microeng.* **2016**, *26*, 107001.
38. P, Liu; Z, Lv; B, Sun; Y, Gao; W, Qi; Y, Xu; L, Chen; L, Wang; C, Ge; S, Li. A universal bonding method for preparation of microfluidic biosensor. *Microfluid Nanofluidics.* **2021**, *25*, 43.
39. A, Koklu; S, Wustoni; V-E, Musteata; D, Ohayon; M, Moser; I, McCulloch; S-P, Nunes; S, Inal. Micro fluidic Integrated Organic Electrochemical Transistor with a Nanoporous Membrane for Amyloid-β Detection. *ACS Nano.* **2021**, *15*, 8130–8141.
40. D, Liang; Y, Huo; Y, Kang; K-X, Wang; A, Gu; M, Tan; Z, Yu; S, Li; J, Jia; X, Bao; S, Wang; Y, Yao; H-S, Philip Wong; S, Fan; Y, Cui; J-S, Harris. Optical Absorption Enhancement in Freestanding GaAs Thin Film Nanopyramid Arrays. *Adv Energy Mater.* **2012**, *2*, 1254-1260.
41. B-Y, Sun; V, Kumar; I, Adesida; J-A, Rogers. Buckled Ribbons of GaAs for Flexible Electronics Buckled and Wavy Ribbons of GaAs for High-Performance Electronics on Elastomeric Substrates. *Adv Mater.* **2006**, *18*, 2857–2862.
42. A-R, Norouzi; A, Nikfarjam; H, Hajghassem. PDMS – PMMA bonding improvement using SiO 2 intermediate layer and its application in fabricating gas micro valves. *Microsyst Technol.* **2018**, *24*, 2727–2736.
43. D, Fuard; T, Tzvetkova-chevolleau; S, Decossas; P, Tracqui; P, Schiavone. Optimization of poly-di-methyl-siloxane (PDMS) substrates for studying cellular adhesion and motility. *Microelectron Eng.* **2008**, *85*, 1289–1293.
44. A, Zahid; B, Dai; R, Hong; D, Zhang. Optical properties study of silicone polymer PDMS substrate surfaces modified by plasma treatment. *Mater. Res Express.* **2017**, *4*, 105301.
45 R, Sivakumar; NY, Lee. Chemically robust succinimide group-assisted irreversible bonding of poly(dimethylsiloxane)–thermoplastic microfluidic devices at room temperature. *Analyst.* **2020**, *145*, 6887–6894
46 Jikai, Xu; Chenxi, Wang; Yanhong, Tian; Bin, Wu; Shang, Wang; and He, Zhang. Glass-on-LiNbO3 heterostructure formed via a two-step plasma activated low-temperature direct bonding method. *Applied Surface Science.* **2018,** 459, 621-629.
47 R, Takigawa; E, Higurashi; T, Asano. Room-temperature wafer bonding of $LiNbO_3$ and SiO_2 using a modified surface activated bonding method. *Jpn. J. Appl. Phys*. **2018**, 57.
48. M-A, Eddings; M-A, Johnson; B-K, Gale. Determining the optimal PDMS – PDMS bonding technique for microfluidic devices. *J. Micromech. Microeng*. **2008**, *18*, 067001.
49. S, Bhattacharya; A, Datta; J-M, Berg; S, Gangopadhyay. Studies on Surface Wettability of Poly (Dimethyl) Siloxane (PDMS) and Glass Under Oxygen-Plasma Treatment and Correlation With Bond Strength. *J Microelectromechanical Syst.* **2005**, *14*, 590–597.
50. R, Sivakumar; K-T-L, Trinh; NY, Lee. Heat and pressure-resistant room temperature irreversible sealing of hybrid PDMS – thermoplastic micro fl uidic devices via carbon – nitrogen covalent bonding and its application in a continuous- flow. *RSC Adv.* **2020**, *10*, 16502.
51. C-W, Tsao; D-L, DeVoe. Bonding of thermoplastic polymer microfluidics. *Microfluid Nanofluid.* **2009**, *6*, 1–16.
52. X, Wen; S, Takahashi; K, Hatakeyama; K-I, Kamei. Evaluation of the Effects of Solvents Used in the Fabrication of Microfluidic Devices on Cell Cultures. *Micromachines* **2021**, *12*, 550.

53. Wu J, Wang R, Yu H, Li G, Xu K, Tien NC, et al. Inkjet-printed microelectrodes on PDMS as biosensors for functionalized microfluidic systems. *Lab Chip*. **2015**, *15*, 690–695.
54. Y, Ren; S-H, Huang; S, Mosser; M-O, Heuschkel; A, Bertsch; P-C, Fraering; J-J, Jason Chen; P, Renaud . A Simple and Reliable PDMS and SU-8 Irreversible Bonding Method and Its Application on a Microfluidic-MEA Device for Neuroscience Research. *Micromachines*. **2015**, *6*, 1923–1934.
55. X, Ye; D, Cai; X, Ruan; A, Cai. Research on the selective adhesion characteristics of polydimethylsiloxane layer. *AIP Adv*. **2018**, *8*, 095004.
56. W-W-Y ,Chow; K-F, Lei; G, Shi; W-J, Li; Q, Huang. Micro Fluidic Channel Fabrication by PDMS-Interface Bonding. *Smart Mater. Struct*. **2006**, *15*, S112.
57. S, Hammami; C, Jean-mistral; F, Jomni and A, Sylvestre. Electrical Conduction in Dielectric Elastomer Transducers. *IEEE Trans. Dielectr. Electr. Insul*. **2020**, *27*, 17–25.
58. M-M-R, Howlader; S, Suehara; T, Suga. Room temperature wafer level glass / glass bonding. *Sensors Actuators A. Phys*. **2006**, *127*, 31–36.
59. S, Schneider; E-J-S, Bras; O, Schneider; K, Schlünder; P, Loskill. Facile Patterning of Thermoplastic Elastomers and Robust Bonding to Glass and Thermoplastics for Microfluidic Cell Culture and Organ-on-Chip. Micromachines **2021**, *12*, 575.